

S.S. Mendigalieva¹, D.A. Birimzhanova¹, I.S. Irgibaeva^{1*},
N.N. Barashkov², Y.E. Sakhno³

¹*L.N. Gumilyov Eurasian National University, Nur-Sultan, Kazakhstan;*

²*Micro Tracers, Inc., San Francisco, California, USA;*

³*University of Delaware, Newark, Delaware, USA*

(*Corresponding author's e-mail: irgsm@mail.ru)

Aggregation-induced emission of 5-(benzylidene)pyrimidine-2,4,6-triones

5-(Benzylidene)pyrimidine-2,4,6-triones with different substituents on the phenyl rings: 5-(4'-dimethylaminobenzylidene) barbituric acid and 5-(4'-methoxybenzylidene) barbituric acid were synthesized, and their spectral-luminescent properties were investigated. A decreasing fluorescence efficiency in the solid-state is general and is mainly attributed to the intermolecular vibronic interactions, which induce the nonradiative deactivation process. Whereas the isolated dye molecules are virtually non-luminescent in dilute solutions, they become highly emissive upon solution thickening or aggregation in poor solvents or in the solid-state, show an increase of luminescence intensity, the phenomenon of the aggregation-induced emission (AIE phenomenon). The development of efficient luminescent materials is a topic of great current interest. The emission color is changed from red (maximum at 630 nm) to green (maximum at 540 nm) by varying the substituent on the phenyl ring from dimethylamino to the methoxy group. Theoretical calculation shows that the dye molecules' aggregation-induced emission characteristics result from intermolecular interactions. Utilizing such features, the molecules can be employed as fluorescent probes for the detection of the ethanol content in aqueous solutions.

Keywords: aggregation-induced emission, barbituric acid, fluorescent probes, fluorescence peak intensities, luminophore, dye molecules, substituent phenyl ring, solid state, intramolecular rotations.

Introduction

Whereas light emissions of luminophores are normally investigated in the solution state, they are practically used as materials commonly in the solid-state [1]. The formation of aggregates with an ordered or random structure in the solid-state is facilitated by the close proximity of molecules that experience strong π - π stacking interactions. The nonradiative decay of the excited state of molecules is often caused by aggregation-caused quenching (ACQ) of light radiation in the condensed phase.

Various chemical, physical, and engineering approaches and processes have been developed to eliminate the effect of ACQ, but attempts have met with only limited success [2].

It would be good if a system can be developed in which light emission is enhanced, rather than quenched, by aggregation because no additional effect will need to be placed to artificially interrupt the very natural process of luminophore aggregation.

Recently, Tang and co-workers found that the fluorescence of some molecules was weak in dilute solutions but became strong when they were in aggregate states [2–4]. The restriction of intramolecular rotation is responsible for such effects. This effect is called Aggregation-Induced Emission (AIE). Utilizing the AIE characteristics, many authors explored potential applications of the AIE luminogens as chemical sensors [5], biological probes [6, 7], smart nanomaterials [8–10], and solid-state emitters [11–15].

We are interested in expanding the AIE system to cover the whole visible spectral region. In this work, we designed and synthesized two derivatives of barbituric acid (Figure 1) and reported their AIE effect. Firstly, the AIE in derivatives of barbituric acid was reported by Barashkov, Bolotin, and Tang in 2004 [16]. Later, these derivatives became the subjects of the number of publications [17, 18]. By changing the substituent on the phenyl group, the conjugation and hence the emission color of the luminophore can be varied. The molecules can be employed as fluorescent probes and can detect the ethanol contents in ethanol-water mixtures [19–23].

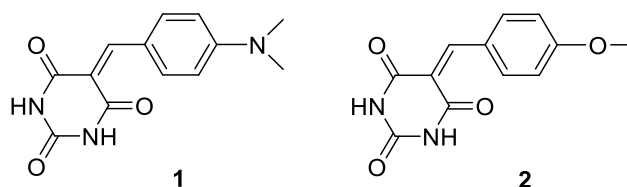


Figure 1. Molecular structures of the pyrimidine-2,4,6-triones derivatives 1 and 2

Experimental

Materials and Instrumentation. Tetrahydrofuran (THF; Labscan), methanol (RDH), *N,N*-dimethylformamide (DMF, Labscan), and other solvents were used as received without further purification. Barbituric acid (pyrimidine-2,4,6-trione), 4-dimethylaminobenzaldehyde, 4-methoxybenzaldehyde were purchased from Aldrich and used without further treatment.

UV absorption spectra were measured on a Milton Roy Spectronic 3000 Array spectrophotometer. Photoluminescence (PL) spectra were recorded on Perkin Elmer LS 55 Fluorescence spectrometer or Hitachi Fluorescence Spectrophotometer F-2000. Particle size measurements were performed on a Beckman Coulter Delsa 440SX Zeta potential analyzer. Scanning electron microscope (SEM) image was taken on a JEOL JSM-7500F electron microscope.

Synthesis. Dye **1** and **2**, namely 5-[(4-dimethylamino)benzylidene]pyrimidine-2,4,6-trione and 5-[(4-methoxy)benzylidene]pyrimidine-2,4,6-trione, were prepared by coupling reaction of barbituric acid with 4-dimethylaminobenzaldehyde and 4-methoxybenzaldehyde in an ethanol solution of sodium hydroxide (Scheme 1). A typical procedure for the synthesis of **1** is given below.

8.96 g (0.07 mol) barbituric acid, 120 mL ethanol, 11.92 g (0.08 mol) 4-dimethylaminobenzaldehyde and 1.2 mL 10 % aqueous solution of sodium hydroxide were added into a 250 mL round-bottom flask. After stirring for 4 h at 80–85 °C, the solution was filtered. The residue was washed with hot water and then ethanol, and dried in vacuum. Dye **1** was obtained as red powder with a yield of 88 %. ¹H NMR (400 MHz, DMSO-*d*₆), δ (ppm): 3.12 (s, 6H), 6.80 (d, 2H), 8.15 (s, 1H), 8.42 (d, 2H), 10.92 (s, 1H), 11.03 (s, 1H). ¹³C NMR (100 MHz, DMSO-*d*₆), δ (ppm): 39.71, 109.53, 111.20, 119.98, 139.05, 150.31, 154.18, 155.48, 162.70, 164.70. Dye **2** was prepared similarly from 8.96 g (0.07 mol) of barbituric acid and 10.88 g (0.08 mol) of 4-methoxybenzaldehyde and isolated as yellow-green powder with a yield of 86 %. ¹H NMR (400 MHz, DMSO-*d*₆), δ (ppm): 3.86 (s, 3H), 7.15 (d, 2H), 8.43 (d, 2H), 8.24 (s, 1H), 11.04 (s, 1H), 11.17 (s, 1H). ¹³C NMR (100 MHz, DMSO-*d*₆), δ (ppm): 55.70, 113.95, 115.54, 125.16, 137.48, 150.20, 154.98, 162.17, 163.46, 163.92.

Results and Discussion

Synthesis and Absorption. To enrich the family of AIE-active molecules, we obtained two pyrimidine-2,4,6-triones (**1** and **2**) with different substituents on the phenyl rings according to Figure 1. While the dye-containing dimethylamino group appears red, that with methoxy substituent is greenish-yellow.

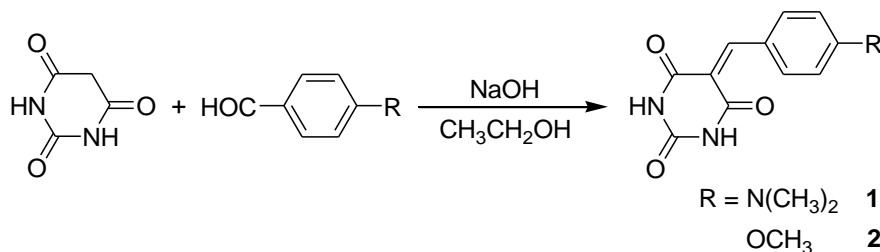
Figure 1. Synthesis of dye **1** and **2**

Figure 2 shows the absorption spectra of **1** and **2** in different solvents. In chloroform, **1** absorbs at 468 nm. The spectrum shifts to shorter wavelengths when the solvent is changed to ethyl acetate and THF. In methanol, the absorption maximum (λ_{ab}) is located at a wavelength similar to that in chloroform. To correlate the position of the λ_{ab} with the solvent, we performed additional measurements and checked the orientation polarizabilities (Δf) of the solvents. The results are summarized in Table 1. In solvents with “lower” and

“higher” polarities, such as chloroform and methanol, **1** shows redder absorption. Since **1** has a high dipole moment, it can be better solvated in highly polar solvents. The good solvation of the molecule enables better planarity and hence shifts the λ_{ab} to the longer wavelengths. On the contrary, the solvating ability of chloroform is comparatively less, but it disturbs little the hydrogen bonding between molecules of **1**. Thus, the λ_{ab} is found in the redder region. A similar change in the absorption behavior with the solvent polarity is also observed in **2**. The λ_{ab} is located at much shorter wavelengths because the electron-donating ability of the methoxy group of **2** is weaker than the dimethylamino moiety in **1**, which has thus lowered its conjugation.

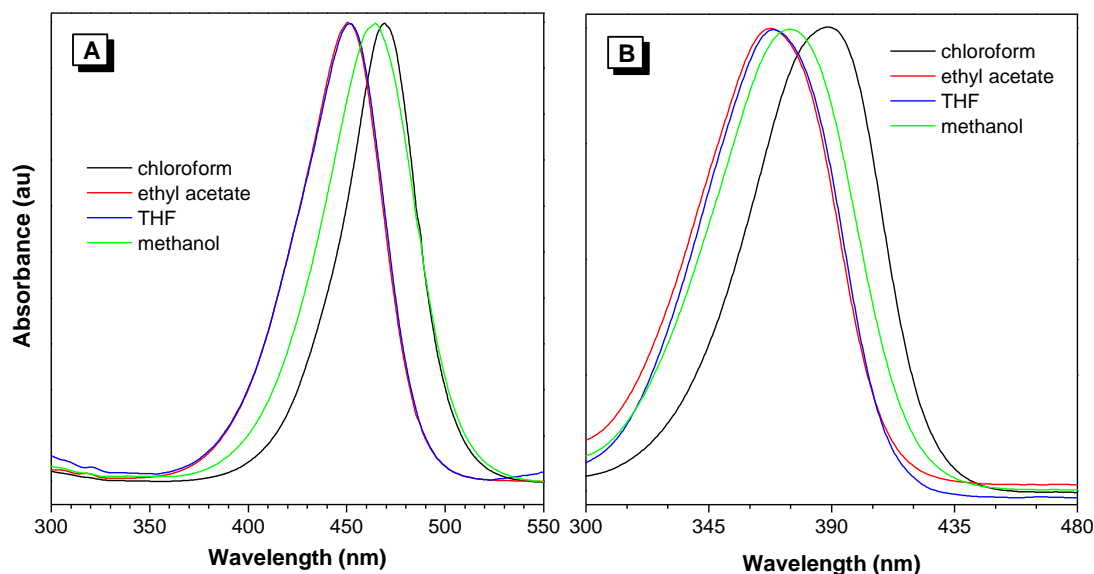


Figure 2. UV spectra of (A) **1** and (B) **2** in different solvents. Concentration: 25 μ M.

Table 1

Absorption of **1 and **2** in Nonhalogenated and Chlorinated Solvents with Different Polarities^a**

Solvent	Δf	λ_{ab} (nm)	
		1	2
Ethyl acetate	0.199	450	367
THF	0.210	452	368
DMF	0.275	460	370
Acetonitrile	0.305	461	372
Methanol	0.308	465	375
Chloroform	0.148	468	388

Note: ^a In solutions with a dye concentration of 25 μ M.

Abbreviation: λ_{ab} = absorption maximum, Δf = orientation polarizability = $[(\epsilon - 1)/(2\epsilon + 1)]/[(\eta^2 - 1)/(2\eta^2 + 1)]$ (ϵ and η are the dielectric constant and refractive index of the solvent) [16, 17].

Light Emission. We then investigated the photoluminescence (PL) of **1** in different organic solvents. In chloroform, **1** exhibits a weak emission at 535 and 630 nm, which can hardly be observed (Figure 3). In more polar solvents, such as THF and methanol, the PL spectrum varies little but displays only broadband at 507 and 539 nm, respectively. The small influence of solvent polarity on the luminescence of **1** suggests that its dipole is too small and leads to a normal π - π^* instead of an intramolecular charge transfer singlet-excited state observed in highly polarized molecules.

The peak at 630 nm in chloroform is due to the aggregate emission of **1** because it is intensified when the solution is concentrated (Figure 2B). The absence of such emission in THF and methanol suggests that **1** is still molecularly dissolved in the solutions. A much higher dye concentration is required for aggregate formation in these solvents.

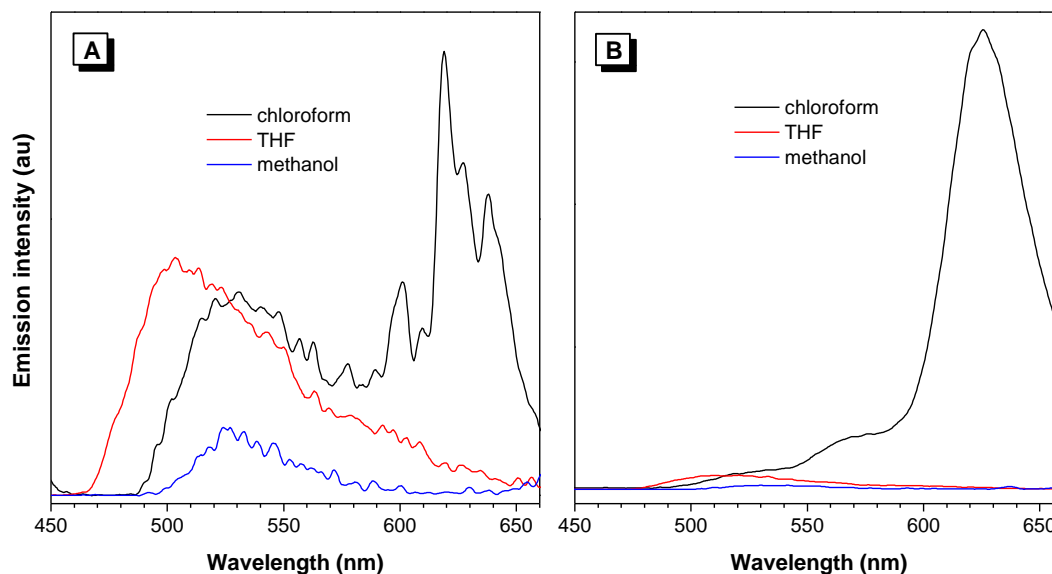


Figure 3. Photoluminescence spectra of **1** in different solvents.
Concentration (μM): (A) 5 and (B) 10. Excitation wavelength: 350 nm

To have a more detailed investigation, we prepared solutions of **1** in THF with different concentrations and measured the PL change (Figure 4). When the solution concentration becomes higher, the broad peak centered at ~ 500 nm is intensified and progressively shifts to the longer wavelengths. At a concentration of $250 \mu\text{M}$, the PL is located at 628 nm, which is 100 nm red-shift from that at $100 \mu\text{M}$. The peak intensity is 10-fold higher, revealing that the emission of **1** is enhanced instead of quenched by aggregate formation. In other words, **1** displays a phenomenon of aggregation-induced emission (AIE). Dye **2** is also AIE-active. In chloroform, it emits at 552 nm, which intensifies when the solution concentration is increased (Figure 5).

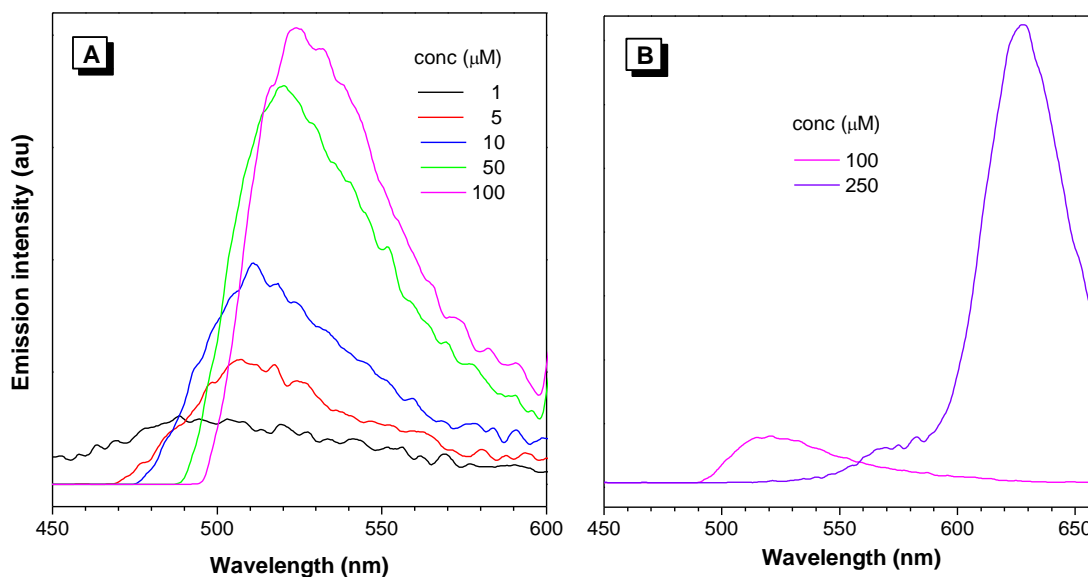


Figure 4. Photoluminescence spectra of THF solutions of **1** with different concentrations.
Excitation wavelength: 350 nm

All the above data indicate that **1** and **2** emit weakly in the dilute solutions but become strong emitters upon aggregation in concentrated solutions [24, 25]. If so, they should also emit intensely in the solid state, since the molecules are in close vicinity in the condensed phase. As expected, powders **1** and **2** give strong red and green lights upon photoexcitation, whose emission maxima are located at the same wavelengths as in concentrated solutions (Figure 6).

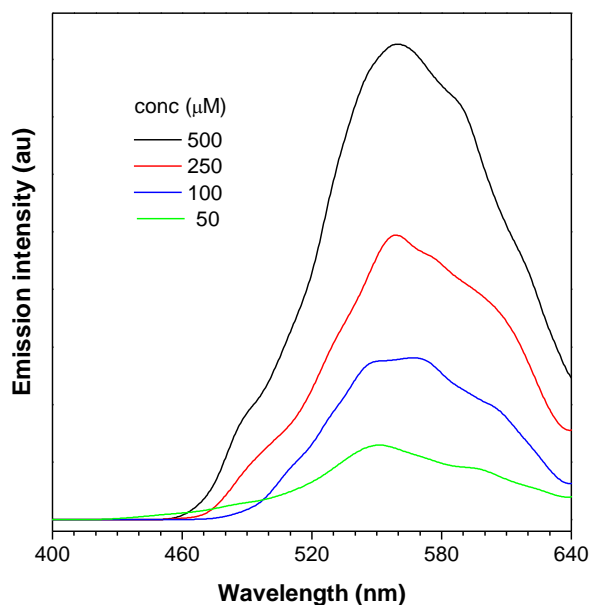


Figure 5. Photoluminescence spectra of chloroform solutions of **2** with different concentrations. Excitation wavelength: 330 nm

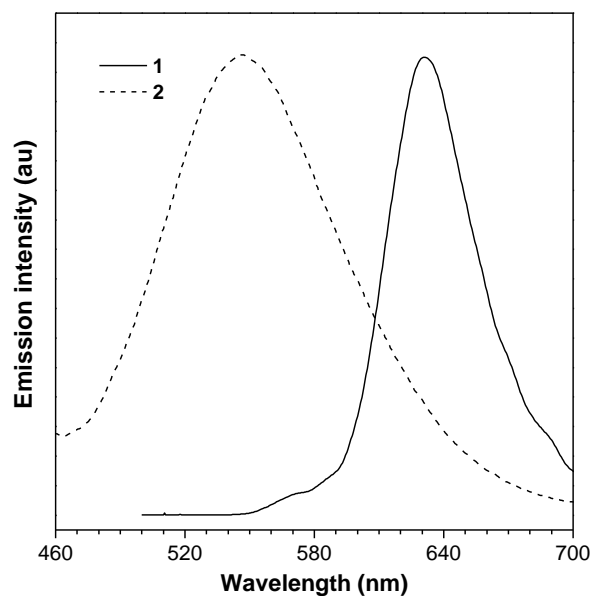


Figure 6. Emission spectra of solid powders of **1** and **2**. Excitation wavelength (nm): 452 (**1**), 368 (**2**)

Figure 7 shows the visual observations of THF solutions and solid powders of **1** and **2** under UV irradiation. Whereas the THF solutions of **1** and **2** are transparent, strong red and green emissions are observed in their solid powders.

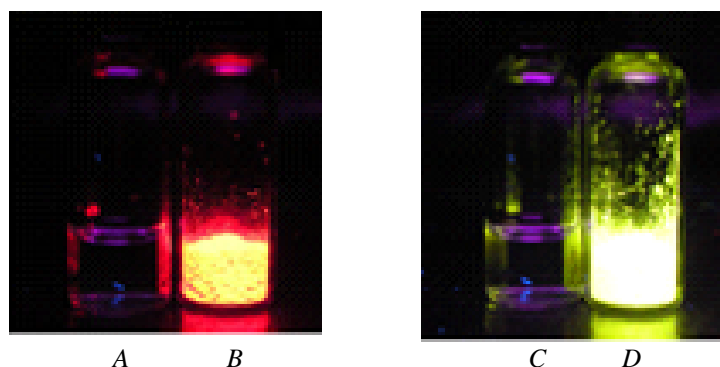


Figure 7. Photographs of (A and C) dilute THF solutions and (B and D) solid powders of **1** (left) and **2** (right) taken under UV light

To determine **1** and **2** are AIE-active, we added water into their THF solutions and studied their PL. Since water does not dissolve **1** and **2**, the dye molecules should be aggregated in THF/water mixtures with high water fractions. Figure 8A depicts the PL spectra of **1** in THF/water mixtures with different water contents. The emission of the solution is enhanced in water and reaches its maximum intensity at 60 % water content (Figure 8B). However, a further increase in the amount of water led to a decrease in the PL intensity, probably due to the change in the packing order of the aggregates from a crystalline to an amorphous state. In the mixture with “lower” water content, the molecules of **1** can slowly assemble in an ordered manner to form more emissive crystalline clusters. In contrast, the dye molecules can abruptly agglomerate in the mixture with a very high water fraction to form less emissive amorphous powders.

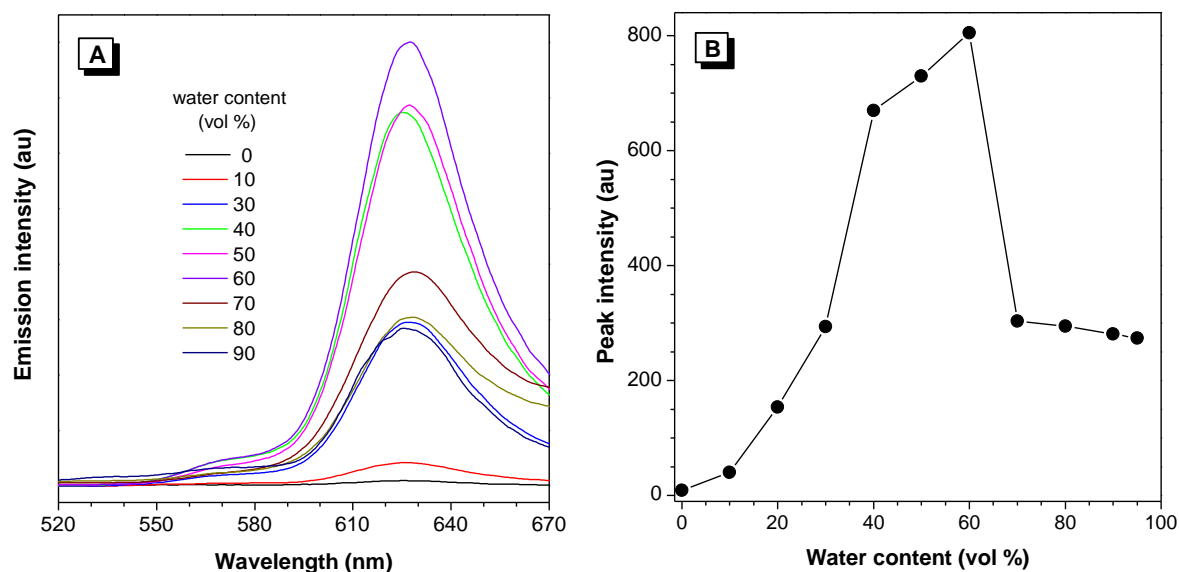


Figure 8. (A) Photoluminescence spectra of **1** in THF/water mixtures with different water contents. (B) Plot of fluorescence peak intensities versus water contents in THF/water mixtures. Concentration: 2.5×10^{-3} M; excitation wavelength: 350 nm

The PL of **2** in THF also becomes stronger when water is added. The peak intensity remains almost unchanged in the presence of up to 70 % water in the solvent mixture, but after that, it starts to increase rapidly (Figure 9). At 90 % water content, the intensity is more than 800 times higher than that of a pure THF solution. Similar to **1**, the emission becomes weaker as more water is added.

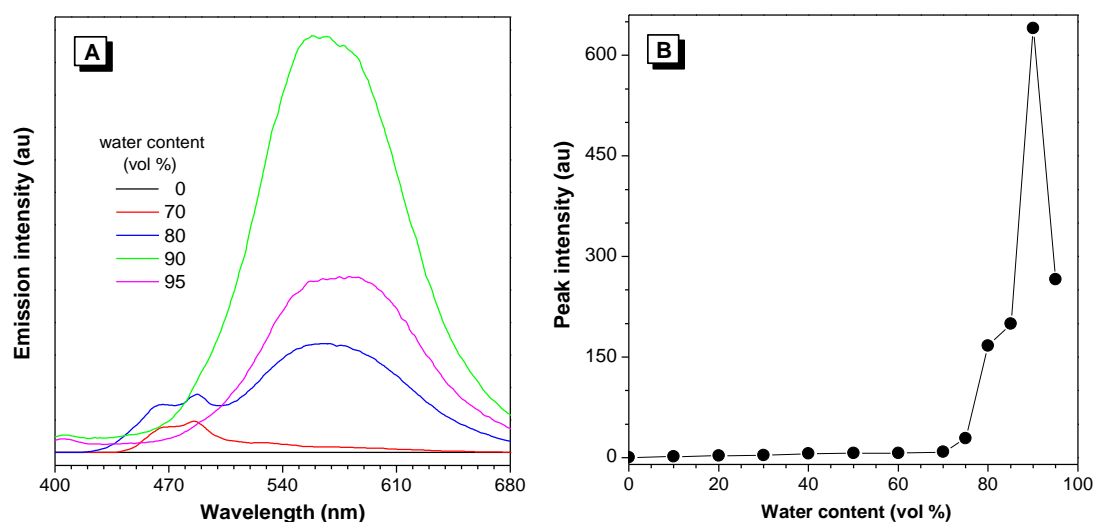


Figure 9. (A) PL spectra of **2** in THF/water mixtures with different water fractions. (B) Plot of fluorescence peak intensities versus water contents in THF/water mixtures. Concentration: 5×10^{-3} M; excitation wavelength: 368 nm

As shown in Figures 8, 9, the emission intensity of solutions **1** and **2** rises with an increase in the concentration of the non-solvent, while the wavelength of the maximum of the luminescence remains unchanged. This is the main difference between the AEE effect and the solvatochromism effect, in which the luminescence wavelength changes with an increase in the concentration of the non-solvent [26, 27].

It should be noted that even at water content as high as 90 %, the THF/water mixtures **1** and **2** remain visually transparent and macroscopically homogeneous. This suggests that the aggregates of molecules should be nanosized. Indeed, we measured the aggregate sizes and found that the particles of **1** and **2** in THF/water mixtures with 90 % water are in the range of 140–200 nm (Figure 10).

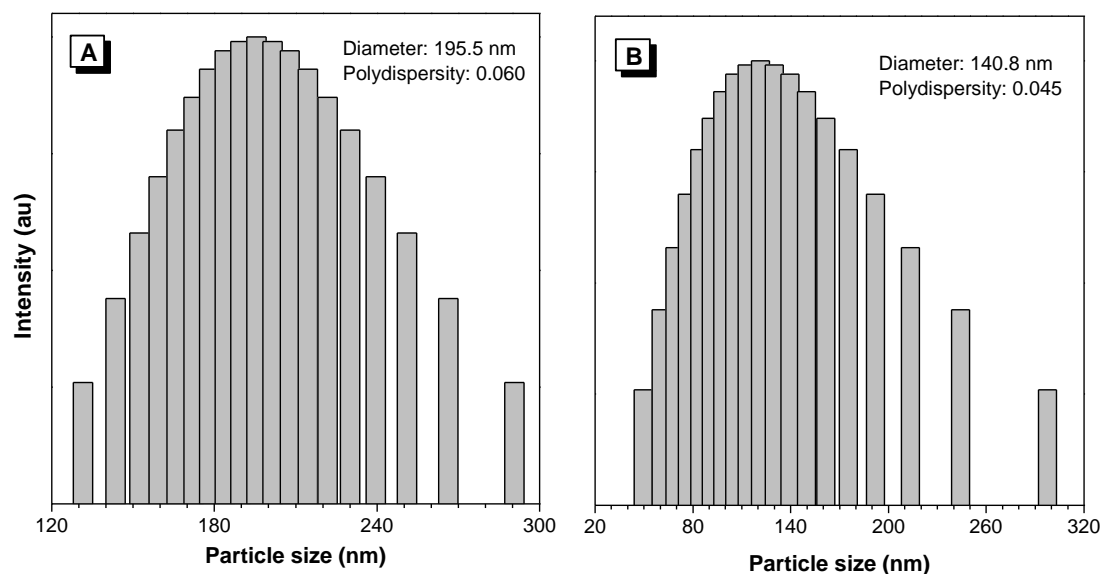


Figure 10. Particle distributions of (A) **1** and (B) **2** in THF/water mixtures with 90 % water. Concentration: 10^{-3} M

Mechanism. For some molecules, such as siloles, the AIE feature is believed to be the result of intramolecular rotation restriction, which shuts down nonradiative relaxation processes and thus boosts their PL emissions. To evaluate this possibility, we doped **1** and **2** into poly(methyl methacrylate) films (1 %), which function as a kind of solid solvent to separate the dye molecules and impede molecular motions at the same time. PL signals cannot be captured from the doped films. Thus, in contrast to their silole congeners, the AIE feature of **1** and **2** should result from intermolecular interactions rather than the restriction of intramolecular rotations.

We carried out quantum chemical calculations using the ZINDO method to further study the structures and optical properties of the dye molecules. Figure 11 shows a sandwich model of an aggregate of **1** formed by intermolecular hydrogen bonds and donor-acceptor interactions. The preferred distance between molecules of **1** in the same plane is 2.6 Å, indicating the existence of strong edge-to-edge interaction or *J*-aggregation. The HOMO is mainly located on the dimethylamino group, while the LUMO is situated on the pyrimidine-2,4,6-trione ring. The absorption band undergoes a bathochromic shift when more molecules are clustered together. For instance, the aggregate formed by 10 molecules of **1** absorbs at 442 nm, close to its experimental value.

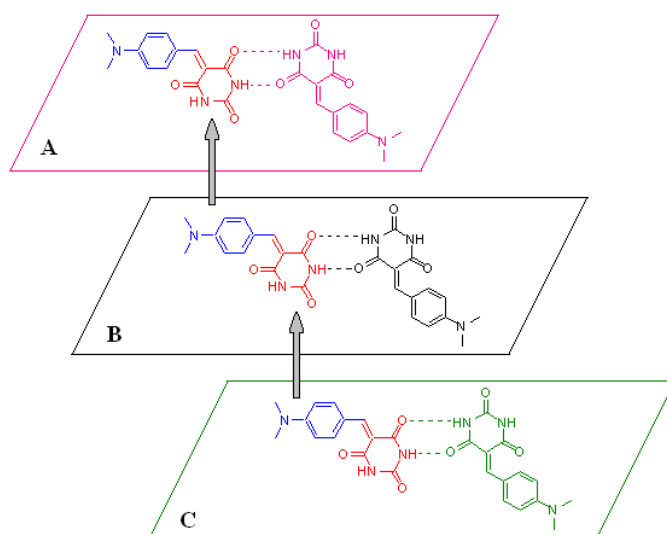


Figure 11. Aggregate formation of molecules **1** via intermolecular hydrogen bonds and D-A interactions in different planes (A, B, and C)

Fluorescence probe. The AIE characteristic has encouraged us to use it as a fluorescent probe to detect the ethanol content in water solution [16]. Since **1** is slightly soluble in ethanol, we prepared a solution of **1** in *N*-methylpyrrolidone and investigated the PL change by adding ethanol/water mixtures with varying ethanol content. The emission intensity increases when the mixture's ethanol fraction is changed from 67 to 40 % (Figure 12). This is understandable since the solvation of the solution becomes poorer progressively, which encourages the aggregation of the molecules of **1**. Through such measurements, a linear dependence of the fluorescence intensity on the ethanol content was established (Figure 12B).

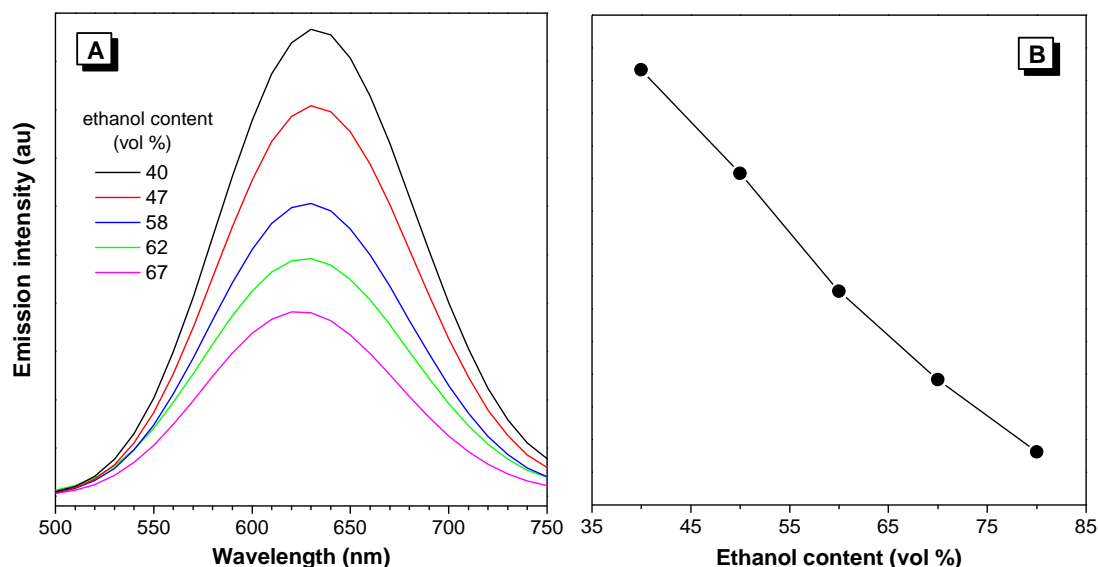


Figure 12. (A) Change in photoluminescence of **1** in *N*-methylpyrrolidone solution upon addition of ethanol/water mixtures with different ethanol contents. Concentration of **1**: 0.13 %; excitation wavelength: 405 nm. The ratio between *N*-methylpyrrolidone and ethanol/water mixture was kept at 3:1 by weight in all measurements. (B) Dependence of fluorescence intensity at 644 nm on the ethanol contents for ethanol/water mixtures

Conclusions

In this work, 5-(benzylidene)pyrimidine-2,4,6-triones with different substituents on the phenyl rings were synthesized, and their optical properties were investigated. Whereas the isolated molecules of **1** and **2** are virtually non-luminescent in dilute solutions, they become highly emissive upon solution thickening or aggregation in poor solvents or the solid-state, demonstrating the AIE phenomenon. The color of the AIE of the dye molecules can be varied by changing the substituent on the phenyl ring. While **1** with a dimethylamino group exhibits red emission, the molecule substituted with methoxy functionality (i.e., **2**) emits green light upon photoexcitation. Analysis by theoretical calculation reveals the strong dependence of the emission of **1** and **2** on their molecular packing. The dye molecules can act as a fluorescent probe and determine the ethanol content in an aqueous solution.

Acknowledgments

The author are grateful to Professor Ben Zhong Tang and his colleagues from the Department of Chemistry, Hong Kong University of Science & Technology for their help in performing this study.

References

- 1 Birks, J.B. (1970). *Photophysics of Aromatic Molecules*. Wiley-VCH Verlag GmbH & Co. KGaA, Vol. 74, 704 pp. <https://doi.org/10.1002/bbpc.19700741223>
- 2 Luo, J., Xie, Z., Lam, J.W.Y., Cheng, L., Chen, H., Qiu, C., Kwok, H.S., Zhan, X., Liu, Y., Zhu, D., & Tang, B.Z. (2001). Aggregation-induced emission of 1-methyl-1,2,3,4,5-pentaphenylsilole. *Chem. Commun.* 2001, 18, 1740–1741. <https://doi.org/10.1039/B105159H>

- 3 Hong, Y., Lam, J.W.Y., & Tang, B.Z. (2011). Aggregation-induced emission. *Chem. Soc. Rev.*, *40* (11), 5361–5388. <https://doi.org/10.1039/C1CS15113D>
- 4 Liu, Y., Tang, Y., Barashkov, N.N., Irgibaeva, I.S., Lam, J.W.Y., Hu, R., Birimzhanova, D., Yu, Y., & Tang, B.Z. (2010). Fluorescent chemosensor for detection and quantitation of carbon dioxide gas. *J. Am. Chem. Soc.*, *132*, 13951–13953. <https://doi.org/10.1021/ja103947j>
- 5 Shi, W., Zhao, S., Su, Y., Hui, Y., & Xie, Z. (2016). Barbituric acid-triphenylamine adduct as an AIEE-type molecule and optical probe for mercury (II). *New J. Chem.*, *40* (9), 7814–7820. <https://doi.org/10.1039/C6NJ00894A>
- 6 Korneev, O.V., Sakhno, T.V., & Korotkova, I.V. (2019). Nanoparticles-based photosensitizers with effect of aggregation-induced emission. *Biopolymers and Cell. Vol. 35. N 4.* 249–267 doi: <http://dx.doi.org/10.7124/bc.000A08>
- 7 Zhang, H., Guo, L., Xie, Z., Xin, X., Sun, D., & Yuan, S. (2016). Tunable aggregation-induced emission of polyoxometalates via amino acid-directed self-assembly and their application in detecting dopamine. *Langmuir*, *32* (51), 13736–13745. <https://doi.org/10.1021/acs.langmuir.6b03709>
- 8 Liang, G.D., Weng, L.-T., Lam, J.W.Y., Qin, W., & Tang, B.Z. (2014). Crystallization-induced hybrid nano-sheets of fluorescent polymers with aggregation-induced emission characteristics for sensitive explosive detection. *ACS Macro Lett.*, *3* (1), 21–25. <https://doi.org/10.1021/mz4005887>
- 9 Wang, X., Song, P., Peng, L., Tong, A., & Xiang, Y. (2016). Aggregation-induced emission luminogen-embedded silica nanoparticles containing DNA aptamers for targeted cell imaging. *ACS Appl. Mater. Interfaces*, *8* (1), 609–616. <https://doi.org/10.1021/acsami.5b09644>
- 10 Goswami, N., Yao, Q., Luo, Z., Li, J., Chen, T., & Xie, J. (2016). Luminescent metal nanoclusters with aggregation-induced emission. *J. Phys. Chem. Lett.*, *7* (6), 962–975. <https://doi.org/10.1021/acs.jpcclett.5b02765>
- 11 Mei, Ju., Leung, Nelson Lik Ching., Kwok, Tsz Kin., Lam, Wing Yip., & Tang, Benzong (2015). Aggregation-Induced Emission: Together We Shine, United We Soar! *Chemical Reviews*, *115*, (21), 11718–11940. <https://doi.org/10.1021/acs.chemrev.5b00263>
- 12 Yuan, W.Z., Yu, Z.-Q., Tang, Y., Lam, J.W.Y., Xie, N., Lu, P., Chen, E.-Q., & Tang, B.Z. (2011). High solid-state efficiency fluorescent main chain liquid crystalline polytriazoles with aggregation-induced emission characteristics. *Macromolecules*, *44* (24), 9618–9628. <https://doi.org/10.1021/ma2021979>
- 13 Marafie, J.A., Bradley, D.D.C., & Williams, C.K. (2017). Thermally stable zinc disalphen macrocycles showing solid-state and aggregation-induced enhanced emission. (2017). *Inorg. Chem.*, *56* (10), 5688–5695. <https://doi.org/10.1021/acs.inorgchem.7b00300>
- 14 An, P., Shi, Z.-F., Dou, W., Cao, X.-P., & Zhang, H.-L. (2010). Synthesis of 1,4-bis[2,2-bis(4-alkoxyphenyl)vinyl]benzenes and side chain modulation of their solid-state emission. *Org. Lett.*, *12* (19), 4364–4367. <https://doi.org/10.1021/ol101847w>
- 15 Zhang, P., Liu, W., Niu, G., Xiao, H., Wang, M., Ge, J., Wu, J., Zhang, H., Li, Y., & Wang, P. (2017). Coumarin-based boron complexes with aggregation-induced emission. *J. Org. Chem.*, *82* (7), 3456–3462. <https://doi.org/10.1021/acs.joc.6b02852>
- 16 Barashkov, N., Bolotin, B., Tang, B., Peng, H., & Chen, J. (2004). *U.S. Patent No. 20040157334 (A1)*.
- 17 Wang, E., Lam, J.W.Y., Hu, R., Zhang, C., Zhao, Y.S., & Tang, B.Z. (2014). Twisted intramolecular charge transfer, aggregation-induced emission, supramolecular self-assembly and the optical waveguide of barbituric acid-functionalized tetraphenylethene. *J. Mater. Chem. C*, *2* (10), 1801–1807. <https://doi.org/10.1039/C3TC32161D>
- 18 Zhu, Z., Qian, J., Zhao, X., Qin, W., Hu, R., Zhang, H., Li, D., Xu, Z., Tang, B.Z., & He, S. (2016). Stable and size-tunable aggregation-induced emission nanoparticles encapsulated with nanographene oxide and applications in three-photon fluorescence bioimaging. *ACS Nano*, *10* (1), 588–597. <https://doi.org/10.1021/acsnano.5b05606>
- 19 Loboda, O., Minaev, B., Vahtras, O., Schimmelpfennig, B., Ågren, H., & Ruud, K. (2003). Ab initio calculations of zero-field splitting parameters in linear polyacenes. *Chemical physics*, *286* (1), 127–137. DOI: [10.1016/S0301-0104\(02\)00914-X](https://doi.org/10.1016/S0301-0104(02)00914-X)
- 20 Dong, Y., Lam, J.W.Y., Qin, A., Sun, J., Liu, J., Li, Z., Sun, J., Sung, H.H.Y., Williams, I.D., Kwok, H.S., & Tang, B.Z. (2007). Aggregation-induced and crystallization-enhanced emissions of 1,2-diphenyl-3,4-bis(diphenylmethylene)-1-cyclobutene. *Chem. Commun.*, *31*, 3255–3257. <https://doi.org/10.1039/B704794K>
- 21 Qin, A., Jim, C.K.W., Lu, W., Lam, J.W.Y., Häußler, M., Dong, Y., Sung, H.H.Y., Williams, I.D., Wong, G.K.L., & Tang, B.Z. (2007). Click polymerization: facile synthesis of functional poly(aryltriazole)s by metal-free, regioselective 1,3-dipolar polycycloaddition. *Macromolecules*, *40* (7), 2308–2317. <https://doi.org/10.1021/ma062859s>
- 22 Minaev, B., Knuts, S., Ågren, H., & Vahtras, O. (1993). The vibronically induced phosphorescence in benzene. *Chemical physics*, *175* (2-3), 245–254.
- 23 Xu, J., Liu, X., Lv, J., Zhu, M., Huang, C., Zhou, W., Yin, X., Liu, H., Li, Y., & Ye, J. (2008). Morphology transition and aggregation-induced emission of an intramolecular charge-transfer compound. *Langmuir*, *24* (8), 4231–4237. <https://doi.org/10.1021/la703662w>
- 24 Zhang, H.-J., Tian, Y., Tao, F., Yu, W., You, K.-Y., Zhou, L.-R., Su, X., Li, T., & Cui, Y.-Z. (2019). Detection of nitroaromatics based on aggregation induced emission of barbituric acid derivatives. *Spectrochimica Acta Part A: Molecular and Biomolecular Spectroscopy*, *222*, 117168. <https://doi.org/10.1016/j.saa.2019.117168>
- 25 Xi, J., Zhang, H., Xu, Z., Tao, F., & Cui, Y. (2021). Wavelength tuneable barbituric acid derivatives: Synthesis, aggregation-induced emission and nitroaromatic detection. *Journal of Luminescence*, *232*, 117865. doi:10.1016/j.jlumin.2020.117865. <https://doi.org/10.1016/j.jlumin.2020.117865>

26 Hu, R., Gómez-Durán, C.F.A., Lam, J.W.Y., Belmonte-Vázquez, J.L., Deng, C., Chen, S., Ye, R., Peña-Cabrera, E., Zhong, Y., Wong, K.S., & Tang, B.Z. (2012). Synthesis, solvatochromism, aggregation-induced emission and cell imaging of tetraphenylethene-containing BODIPY derivatives with large Stokes shifts. *Chem. Commun.*, 48 (81), 10099–10101. <https://doi.org/10.1039/C2CC35188A>

27 Liu, B., Luo, Z., Si, S., Zhou, X., Pan, C., & Wang, L. (2017). A photostable triphenylamine-based flavonoid dye: solvatochromism, aggregation-induced emission enhancement, fabrication of organic nanodots, and cell imaging applications. *Dye. Pigment.*, 142, 32–38. <https://doi.org/10.1016/j.dyepig.2017.03.023>

С.С. Мендигалиева, Д.А. Биримжанова, И.С. Иргибаетова, Н.Н. Барашков, Ю. Сахно

5-(Бензилиден)пиримидин-2,4,6-триондарының агрегаттық-индукцияланған эмиссиясы

Фенил сақиналарында әртүрлі алмастырғыштары бар 5-(бензилиден)пиримидин-2,4,6-триондардың спектрлік-люминесценттік қасиеттері синтезделді және зерттелді: 5-(4'-диметиламинобензилиден) барбитур қышқылы және 5-(4'-метоксибензилиден) барбитур қышқылы. Қатты күйдегі флуоресценция тиімділігінің төмендеуі өте жалпы сипатқа ие сияқты радиациялық емес дезактивация процестерін тудыратын молекулааралық тербеліс әсерлесуімен түсіндіріледі. Оқшауланған бояғыш молекулалар сұйылтылған ерітінділерде іс жүзінде люминесценцияланбайды, олар ерітінді концентрациясының жоғарылауымен немесе нашар еріткіштерде немесе қатты күйде агрегатталуымен қатты сәуле шығарады, люминесценция қарқындылығының жоғарылауын, агрегаттық-индукцияланған эмиссия құбылысын көрсетеді (АИЭ құбылысы). Тиімді люминесцентті материалдарды әзірлеу өзекті тақырып болып табылады. Фенил сақинасындағы орынбасар диметиламинодан метокситопқа өзгерген кезде сәулелену түсі қызылдан (максимум 630 нм) жасылға (максимум 540 нм) өзгереді. Теориялық есептеу бояғыш молекулалардың агрегаттық-индукцияланған эмиссиясының сипаттамалары молекулааралық өзара әрекеттесудің нәтижесі екенін көрсетеді. Осы қасиеттің арқасында молекулаларды флуоресцентті зондтар ретінде қолдануға болады және сулы ерітінділердегі этанол құрамын анықтауға болады.

Кілт сөздер: агрегаттық-индукцияланған эмиссия, барбитур қышқылы, флуоресцентті зондтар, флуоресценцияның ең жоғары қарқындылығы, фосфор, бояғыш молекулалары, фенил сақинасын алмастырғыш, қатты күй, молекулаішілік айналымдар.

С.С. Мендигалиева, Д.А. Биримжанова, И.С. Иргибаетова, Н.Н. Барашков, Ю.Е. Сахно

Агрегационно-индуцированная эмиссия 5-(бензилиден)пиримидин-2,4,6-трионов

Синтезированы и исследованы спектрально-люминесцентные свойства 5-(бензилиден)пиримидин-2,4,6-трионов с различными заместителями в фенильных кольцах: 5-(4'-диметиламинобензилиден) барбитуровая кислота и 5-(4'-метоксибензилиден) барбитуровая кислота. Снижение эффективности флуоресценции в твердом состоянии носит довольно общий характер и, в основном, объясняется межмолекулярными колебательными взаимодействиями, которые индуцируют процессы безызлучательной дезактивации. Тогда как изолированные молекулы красителя практически не люминесцируют в разбавленных растворах, они становятся сильно излучающими при увеличении концентрации раствора или агрегации в плохих растворителях или в твердом состоянии, проявляют увеличение интенсивности люминесценции, явление агрегационно-индуцированной эмиссии (явление АИЭ). Разработка эффективных люминесцентных материалов является актуальной темой. При изменении заместителя в фенильном кольце с диметиламино- на метоксигруппу цвет излучения меняется с красного (максимум при 630 нм) на зеленый (максимум при 540 нм). Теоретический расчет показывает, что характеристики агрегационно-индуцированной эмиссии молекул красителя являются результатом межмолекулярных взаимодействий. Благодаря этому свойству молекулы можно использовать в качестве флуоресцентных зондов и определять содержание этанола в водных растворах.

Ключевые слова: агрегационно-индуцированная эмиссия, барбитуровая кислота, флуоресцентные зонды, интенсивности пиков флуоресценции, люминофор, молекулы красителя, заместитель фенильного кольца, твердое состояние, внутримолекулярные вращения.

Information about authors

Mendigaliyeva, Svetlana Samigulliyena — 3rd year PhD student, Chemistry Department, L.N. Gumilyov Eurasian National University, Satpayev street, 2, 010000, Nur-Sultan, Kazakhstan; e-mail: svet_men@mail.ru; <https://orcid.org/0000-0002-2737-7188>;

Birimzhanova, Dinara Asylbekovna — PhD in Chemical Sciences, Senior Lecturer, L.N. Gumilyov Eurasian National University, Satpayev street, 2, 010000, Nur-Sultan, Kazakhstan; e-mail: dinarabirimzhanova@gmail.com; <https://orcid.org/0000-0002-5572-9339>;

Irgibaeva, Irina Smailovna (corresponding author) — Doctor of science in chemistry, Professor of Chemistry Department, L.N. Gumilyov Eurasian National University, Satpayev street, 2, 010000, Nur-Sultan, Kazakhstan; e-mail: irgsm@mail.ru; <https://orcid.org/0000-0003-2408-8935>;

Barazhkov, Nikolay Nikolayevich — Doctor of science in chemistry, Director of R&D and Technical Services, Micro-Tracers, Inc. 1370 Van Dyke Avenue San Francisco, CA 94124, USA; e-mail: nikolay@microtracers.com; <https://orcid.org/0000-0003-2494-9248>;

Sakhno, Yuriy Eduardovich — Dr., Postdoctoral Fellow, Department of Plant and Soil Sciences, 154a Townsend Hall, 531 S. College Avenue Newark, DE 19713; University of Delaware, Delaware, USA; e-mail: ysakhno@udel.edu; <https://orcid.org/0000-0001-8115-739X>